J Polym Environ (2018) 26:275–290
DOI 10.1007/s10924-017-0946-0

ORIGINAL PAPER

Investigation of Polypropylene-Montmorillonite Clay Nanocomposite Films Containing a Pro-degradant Additive

A. A. Yussuf[1] · M. A. Al-Saleh[1] · M. M. Al-Samhan[1] · S. T. Al-Enezi[1] · A. H. Al-Banna[1] · G. Abraham[1]

Published online: 3 February 2017

Abstract This paper investigates the performance of polypropylene (PP) incorporated with montmorillonite (MMT) nanoclay, maleic anhydride grafted PP (PP-g-MAH), and pro-degradant additive (TDPA®), which provides additional benefits of increasing biodegradability. A twin-screw extruder was used to compound PP, MMT, PP-g-MAH, and TDPA, and the extruded nanocomposite films were collected for testing, and their mechanical, thermal, barrier, oxo-biodegradability, and morphological properties were evaluated. Tensile test, differential scanning calorimetry (DSC), thermogravimetric analysis (TGA), oxygen permeability test, soil burial test, X-ray diffraction (XRD), transmission electron microscopy (TEM), and scanning electron microscope (SEM) analysis were used to investigate these properties. Increasing MMT content from 1 to 3 phr increases tensile strength and Young's modulus of the neat PP samples up to ca.45% and 27% respectively. Improvement of thermal properties for neat PP samples was observed by increasing MMT content from 1 to 3 phr. However, at 4 phr MMT content, both mechanical and thermal properties of nanocomposites dropped slightly. For soil buried samples, DSC and TGA results revealed significant changes in the thermal properties for PP samples containing TDPE additive compared to neat PP, clearly confirming the effectiveness of this TDPA additive in promoting oxo-biodegradation process of PP. Similarly weight loss evaluation result shows that about 4% weight loss for sample (PP/TD), which is PP and TDPA blend only, compared to neat PP. However, increasing MMT content from 1 to 4 phr slightly reduced weight loss of PP from 3.5 to 1.5%, respectively, for 6 month soil exposure period, which indicates that increasing MMT content was detrimental to the degradation process. For higher MMT content, the oxygen permeability of PP nanocomposites was decreased by 46% of the corresponding values for neat PP. The XRD and TEM results confirmed the exfoliation structure of the nanocomposites. The morphological change after soil burial test was studied using scanning electron microscopy (SEM).

Keywords Nanocomposite · Oxo-biodegradation · Thermal properties · Pro-degradant additive · Barrier properties

Introduction

Polypropylene (PP) is one of the largest volume plastic produced in the world and fastest growing thermoplastics in terms of market shares, and it has significantly penetrated numerous sectors of manufacturing such as in the area of medical, automotive, and packing industries [1, 2]. This commercial importance of PP is mainly attributed to its cost-effectiveness, good mechanical properties, and ease in processing [3]. Packaging with improved barrier properties has great importance in food packaging industries as it extends the shelf life of food by preventing humidity and oxygen [4–7]. Therefore, to overcome the disadvantages of PP, such as low barrier properties, low service temperature, and low toughness, many researchers have tried to improve those properties by incorporating layered nanoparticles such as layered silica and organoclay [8–14]; these nanofillers have attracted great scientific and technological interest due to their potentiality to exhibit new characteristics that

✉ A. A. Yussuf
aayussuf@gmail.com

[1] Polymeric Products and Customization Program, Petroleum Research Center, Kuwait Institute for Scientific Research, P.O. Box 24885, Safat 13109, Kuwait

cannot be achieved with micromaterials. Among nanofillers employed for nanocomposite preparation, nanoclay is vastly used due to its unique structure with a high aspect ratio and its natural abundance [15]. The most common nanoclay material predominantly utilized in the polymer clay nanocomposites is montmorillonite (MMT). The incorporation of MMT in the polymer in an extruder leads to dispersion of the MMT particles in the polymer matrix in the molten state, providing significant improvements in polymer properties [15]. However, compatibilization is a key issue into improving the properties of nanocomposites; this is due to the lack of strong interface between the polymer matrix and nanoclay [16].

Recent achievements in nanocomposite technology have fueled the need for new knowledge and findings in the field of polymer nanocomposites resulting in the development of respective polymer nanocomposites: polypropylene/polylactic acid [4], polypropylene [17–21], polylactic acid [22–24], polyethylene terephthalate [25], and polystyrene [26]. For the past few years, many studies have been done in the field of PP nanocomposites [8, 10–12, 19, 21] based on layered silicates, such as MMT, which has gained tremendous popularity among scientists and industries, this is due to the wide application of PP nanocomposites in commodity and engineering applications. Many researchers [19, 27] have reported increased thermal stability of nanocomposites in relation to PP in the presence of an organoclay. Others have reported the influence of processing conditions and clay type on nanostructure [28, 29], and chemical treatment and modifications [17, 30]. PP nanocomposites constitute the most important material for packaging due to low cost, excellent processability, and enhanced thermal and mechanical properties. However, they have been a target of much criticism due to their lack of degradability, representing a serious global environmental problem, and this is the biggest concern for many food packaging industries. New bio-based or biodegradable polymers, such as polylactic acid (PLA) and polycaprolactone (PCL), have been exploited to develop biodegradable nanocomposites [22, 23, 31] for reducing packaging waste. However, the use of biodegradable polymers has been limited because of problems related to performances (brittleness, poor moisture barrier), processing (low heat distortion temperature), and cost.

The possible alternative approach is the use of commercially available pro-degradant additives, which makes polyolefins oxo-biodegradable by breaking down the long chain of polyolefin into a small molecular weight, where eventually the pro-degradant additives can completely degrade the polymer with the action of sunlight [32]. Hence, degradable PP can be obtained using special pro-oxidant/pro-degradants additives that can contain various active components, metal strearates (Fe, Ce, Co), and citric acid. This degradation mechanism is called oxo-degradation, which is basically a two-stage process of initial oxidative degradation followed by the biodegradation of the product [32]. The oxo-degradation process of polyethylene with pro-oxidant/pro-degradant additives has been reported extensively in literature [33–35]. Some work on PP has been done by researchers [36, 37] using pro-degradant additive, who investigated the degradation process under accelerated test conditions and evaluated the effect of pro-degradant additive on the degradation rate of PP. Significant changes in the morphological and thermal properties were reported with PP samples containing pro-degradant additive compare to pure PP [37]. However, the use of this additive in PP is not fully exploited, particularly using with nanoclay fillers as an added value to enhance and improve other properties such as mechanical, thermal, and barrier properties for packaging application. To the best of our knowledge oxo-degradation of PP nanocomposites blended with pro-degradant additive has not been reported openly in literature.

Therefore, the main goal of this study is to investigate the combination of PP-MMT nanocomposites blended with commercially available pro-degradant additive (TDPA), and to evaluate its performance in terms of mechanical, thermal, barrier, oxo-biodegradability and morphological properties; and particularly to assess the effect of TDPA additive on PP degradation process.

Experimental

Materials

The grade of PP used was HF029 produced by EQUATE petrochemical company (Kuwait). The homopolymer PP has a melt flow index of 2.9 g/10 min (2.16 kg at 230 °C). The organoclay (Nanomer 1.30TC), Montmorillonite (MMT), was obtained from Nanocor Inc. Arlington Heights IL, USA, it was a white powder organically modified with octadecylamine with mean dry particle size of 16–22 μm. The oxo-biodegradable additive, pro-degradant, TDPA® (Totally Degradable Plastic Additive), in pellet form was supplied by EPI Environmental Technologies and Products Inc., and only 3 wt% of TDPA was used as recommended by the supplier. This TDPA additive utilizes a combination of transition metal carboxylate and hydro-carboxylic acids, and the main carboxylates are cerium, cobalt, and iron stearate; for instance, iron is recognized as photo-initiating, whereas cobalt (nickel and copper) is sensitive to thermal activation [32]. The grade of PP-g-MAH as a compatibiliser with a maleic anhydride content of 1%, Orevac CA 100 from Atofina, was used to improve the compatibility of PP nanocomposites.

Preparations of Nanocomposites

All samples, PP and nanocomposites, were prepared with twin screw extruder (model Laptch LTE26/40, Lab Tech Engineering), co-rotating screws (L/D = 40). Polymer pellets were dried at 40 °C for 24 h prior to compounding, while the nanoclay was dried at 50 °C for 3 h in air-circulated oven prior to compounding to remove moisture. PP, TDPA, and PP-g-MAH blends were prepared with weight percentage (wt %), while MMT was added as parts per hundred (phr) in the blends [24]. Designation of materials and their compositions are shown in Table 1. The barrel temperature profile adopted during compounding of all the blends was 220 °C at the feed section decreasing to 200 °C at the die head. The screw speed of the extruder was fixed at 45 rpm. The extruded films were produced using thin film die head machine with a barrel temperature of 200 °C. Samples were cut by using dumbbell shape according ASTM D638 standard. All test specimens were allowed to condition under ambient conditions in desiccators for at least 24 h prior to testing.

Characterization

Mechanical Properties

Tensile test was carried out according to ASTM D 638, using Testometric tensile testing machine (model M250) under ambient conditions with crosshead speeds of 50 mm/min. Mechanical properties, such as tensile strength and Young's modulus, were collected for the evaluation of PP and its nanocomposite films.

Table 1 Designation of materials and their compositions

Sample Designations	PP (wt%)	PP-g-MAH (wt%)	TDPA (wt%)	MMT (phr)
PP	100	–	–	–
PP/MA*	95	5	–	–
PP/TD	97	–	3	–
PP/MA/TD*	92	5	3	–
PP/MA/M3*	95	5	–	3
PP/MA/TD/M1	92	5	3	1
PP/MA/TD/M2	92	5	3	2
PP/MA/TD/M3	92	5	3	3
PP/MA/TD/M4	92	5	3	4

PP polypropylene, *TD* TDPA, biodegradable additive, *MA* PP-g-MAH, PP grafted maleic anhydride. M_n MMT, montmorillonite, where n = 1, 2, 3, 4

*Additional samples to evaluate the effects of PP-g-MAH, TDPA and MMT

Thermal Properties

Differential Scanning Calorimetry (DSC)

Differential scanning calorimeter (DSC) measurements were carried out using a DSC-50, manufactured by Shimadzu in Japan. The starting temperature was 25 °C and was raised to 300 °C, then cooled down to room temperature under nitrogen atmosphere with 7–10 mg of samples at a heating and cooling rate of 10 °C min^{-1}. Measurements were repeated at least twice with different samples. Thermal properties, such as melting enthalpy ΔH_m melting temperature (T_m), crystallization temperature (T_c) and degree of crystallinity (X_c), were calculated from DSC traces and recorded. The degree of crystallinity (X_c) of the samples was calculated from the melting enthalpy ΔH_m) results for each sample using Eq. (1).

$$\% \text{ Crystallinity } \left(X_c\right) = 100 \times \frac{\Delta H_m}{f \times \Delta H_m^{\circ}} \quad (1)$$

where ΔH_m is the measured melting enthalpy, f is the weight fraction of PP phase, and ΔH_m^o is the enthalpy of 100% crystalline PP, which is 207 J/g [19].

Thermogravimetric (TGA) Thermogravimetric analysis (TGA) is a test that determines the changes in the weight of the material with increase in temperature, and it is a useful technique to study the thermal stability of polymers. Therefore, in order to examine the thermal stability and thermal degradation behavior for all samples both before and after the soil burial degradation process, TGA was performed by using a DTG-60 instrument, manufactured by Shimadzu in Japan. A sample weight of around 10 mg was heated from 25 to 700 °C at a heating rate of 10 °C min^{-1} under nitrogen atmosphere. TGA parameters, such as onset temperature, were directly calculated from TGA traces; it corresponds to the temperature at which the weight loss begins.

Oxo-Biodegradation Test The methodology used for the biodegradation test was based on using a simple soil burial test in order to simulate the oxo-biodegradation of nanocomposite films in a common disposal environment or outdoor exposure [24]. All tests were done according to ASTM D6954-4 standard testing method [32]. This method will evaluate the oxo-biodegradability of PP by monitoring changes in their physical properties due to the action of microorganisms. All film samples were buried in the soil of a garden with composted solid waste materials in a rectangular wooden box, which was kept open at the top to ensure a continuous oxygen supply to the samples, and to have enough high sunlight contact, and also water so that aerobic biodegradation of the organic matter will occur. It was located outside the natural environ-

ment (outdoor exposures) for a total period of 6 months, from May to October; it is worth mentioning that the average temperature here in Kuwait exceeded more than 45 °C daily in the first four months of the testing period. The samples were recovered from the soil at different stages of degradation (2, 4, and 6 months). After the testing time was completed, the compost samples were washed by using running water in order to remove the sand from the surface of the samples. All the samples were dried in the oven at a temperature of 50 °C until the samples reached a constant weight, and then stored in a desiccators at room temperature for further analytical measurements. Biodegradability was assessed and evaluated by measuring weight loss before and after soil burial testing. Also, the surface morphological appearance of the composted samples was evaluated for visual comparison by using SEM. The weight loss of composted samples was calculated using Eq. (2).

$$\% \text{ Weight loss} = \frac{W_i - W_a}{W_i} \times 100 \quad (2)$$

where W_i and W_a are the sample weight before and after the soil burial and composting test, respectively.

Evaluation Technique of Oxygen Permeability Mocon OxTran 2/21 device, manufactured by Modern Controls Inc., was used for oxygen permeability tests in accordance with ASTM D 3985 [38]. It has been extensively used to test the gas barrier properties of films [39]. To conduct the experiment, a continuous flow of gas was maintained on both sides of the produced thin film. First, nitrogen gas was passed over both surfaces of the film in order to remove oxygen from the film. Then, immediately, the nitrogen on one side was replaced by oxygen. Flat films with a thickness of about 100 µm were clamped into the diffusion cell that was purged of residual oxygen, and then pure oxygen was introduced into the system. Molecules of oxygen diffusing through the film to the inside chamber were conveyed to the sensor by the carrier gas. The diffusing oxygen was measured by a sensitive oxygen detector. These experiments were conducted at 23 °C and 0% relative humidity (RH). Three different films were tested for each formulation and the average values were reported.

Morphological Analysis X-ray diffraction (XRD) studies were carried out on a Siemens D5000 X-ray diffractometer. The diffraction patterns were recorded with a step size of 0.02°, from 2θ = 2.0 to 10°. The interlayer distances (d-spacing) of the MMT in the nanocomposites were derived from the peak positions (001 reflection) in the XRD scans, according to Bragg's Eq. (3).

$$\text{d-spacing} = \frac{n\lambda}{\sin\theta} \quad (3)$$

where n is an integer, θ is the diffraction angle giving the primary diffraction peak, and λ is the X-ray wavelength. In these experiments, λ = 0.154 nm (CuKα) and n = 1 were used.

The morphology of the samples, particularly the outer surface of the original samples (before soil burial) and composted samples (soil buried samples for oxo-biodegradability test) were examined and assessed by using Scanning Electron Microscope (SEM), A TESCAN TS5135MM model. The specimens were sputter coated with a thin layer of gold by using vapour deposition techniques to avoid electrostatic charging during sample examination. The image results were analyzed to investigate the influence of the degradation process on the sample surface.

For transmission electron microscopy (TEM), the sample was embedded in Epon resin; and it was then mounted onto ultramicrotome where sections were cut at thickness of 70–100 nm, and sections were collected on 300 mesh copper grids. The sections were examined and observed by a TEM model JEOL 1200XE2 at 100 kV. Finally the micrographs were taken by using soft imaging system software.

Results and Discussion

Mechanical Properties

Table 2 shows the effect of MMT content on mechanical properties such as tensile strength and Young's modulus of all samples. The tensile strength and Young's modulus of the samples are compared to those of neat PP. As shown in Table 2, the tensile strength of the nanocomposite increased as the MMT content increased from 1 to 3 phr. For instance, the tensile strength of neat PP (control) was 33 MPa, while at MMT content of 3 phr the tensile strength was 48 MPa, which showed 15 MPa (ca. 45%) improvement in the tensile strength of the

Table 2 Mechanical properties of PP, PP-additive blends and its nanocomposites

Sample	Tensile strength (MPa)	Young's modulus (MPa)
PP	33 ± 1.5	136 ± 8
PP/MA	35 ± 1.9	138 ± 8
PP/TD	32 ± 1.7	132 ± 7
PP/MA/TD	34 ± 1.8	140 ± 10
PP/MA/TD/M1	39 ± 2.0	147 ± 10
PP/MA/TD/M2	43 ± 2.5	152 ± 11
PP/MA/M3	50 ± 3.0	168 ± 10
PP/MA/TD/M3	48 ± 2.8	172 ± 12
PP/MA/TD/M4	40 ± 1.9	142 ± 10

nanocomposites compared to neat PP and PP/TD samples. The increased tensile strength could be related to exfoliation of the MMT layers in the PP matrix. This behavior is due to the existing stress transfer from matrix to the filler, and there is a strong bond between the filler and the matrix, which would interfere with the stress distribution throughout the composite when load is, applied [40]. However, this increase declined at 4 phr of MMT, which indicates that 3 phr of MMT content could be a satisfactory amount; and also it could be attributed to the decrease of bonding strength between MMT and PP matrix in the composite due to excess MMT loading. On the other hand, the addition of TDPA additive into neat PP, sample (PP/TD), has slightly decreased the mechanical properties of neat PP from 33 to 32 MPa for tensile strength and from 136 to 132 MPa for Young's modulus. This decrease is probably due to the lack of compatibility between PP and TDPA additive; and the absence of MMT nanoclay and PP-g-MAH contents in the blend for this sample (PP/TD), which as a result could cause poor and weak interaction between them. Similar trend of observation was reported in the literature by other researcher [41].

As shown in Table 2, the Young's modulus of neat PP is enhanced by the addition of MMT nanoclay. This increase in Young's modulus could be due to a strong interaction between the PP and MMT nanoclay filler, and this improvement in stiffness was because of the reinforcement effect of the rigid inorganic MMT, which constrains and restricts the molecular motion of PP chains. The enhancement in the modulus of PP/MMT nanocomposites could also be caused by the exfoliation of MMT layers in the PP matrix, which is a delaminating process of nanoclay particles. When the clay particles are dispersed throughout the polymer blend matrix, it could lead to a higher aspect ratio of the silicate layer, and hence, a larger interfacial area. Both the higher aspect ratio and the interfacial area will make the stress transfer to the silicate layers more effective, and subsequently, improve the mechanical properties of the formed nanocomposite materials. It is noted that both tensile strength and Young's modulus of neat PP have been improved by increasing amount of MMT nanoclay content in the PP matrix, similar observation has been reported in the literature by others [42, 43]. However, it is interesting to note a further increase in MMT content to 4 phr decreases Young's modulus of the nanocomposite. This is because as the nanoclay loading increases, the nanoclay formed a cluster and agglomerate among themselves, resulting lower dispersion and poor interface between nanoclay and PP matrix, which could decrease the reinforcement effect as a result. Previous study on polymer nanocomposites by Chung et al. [44] has also reported that the Young's modulus of polymer decreased when the MMT loading exceeds more than 5 wt%.

Furthermore, in order to understand the effect of PP-g-MAH, TDPA and MMT on the mechanical properties, additional data of PP/MA, PP/MA/TD and PP/MA/M3 blends was presented, reported and tabulated also in Table 2. As shown in Table 2, using PP-g-MAH as a compatibilizer, both tensile strength and Young's modulus of PP and PP/TD samples have improved, which could mean that PP-g-MAH leads to better adhesion between PP and additive. However, for samples PP/MA and PP/MA/TD, presence of TDPA additive in the composite resulted increment in the Young's modulus and slight reduction in tensile strength was observed due to polymer matrix plasticization, where TDPA acts as plasticizer. Similar pattern of behavior was observed for samples PP/MA/M3 and PP/MA/TD/M3 with the addition of TDPA additive which improves Young's modulus by 4 MPa and slightly reduces tensile strength by 2 MPa. Hence, increasing the MMT nanoclay filler content in the nanocomposite resulted in enhancement of Young's modulus, which was further improved by the addition of TDPA additive. It is therefore possible that the synergistic effect of MMT, PP-g-MAH and TDPA could promote the better performance of nanocomposites in terms of mechanical properties.

Thermal Properties

Differential Scanning Calorimetry (DSC)

Figures 1 and 2 show the DSC heating and cooling curves respectively for all samples both before and after soil burial. All the results are tabulated in Table 3, which presents the melting temperature (T_m), crystallization temperature (T_C), and degree of crystallinity (X_c) obtained from the DSC analysis for all samples, both original (before soil burial) and after soil burial samples, for a period of 6 months. As shown in Fig. 1a and Table 3, the melting temperature of neat PP slightly increased with the addition of MMT, which means that the crystal size of PP had some change that could increase melting temperature for higher MMT content. The other possible explanation might be the role of the compatibilizer (PP-g-MAH) used, which diffuses into the gallery of silicate layers to the polymer and clay forming more wetted surface and resulting into higher reinforcement for higher melting temperature [45]. However, the DSC result in Fig. 1a reveals a slight decrease in melting point temperature upon the further addition of 4 phr MMT content, which indicates that the composite reaches the saturation point and an agglomeration at higher MMT contents.

As shown in Table 3, the degree of crystallinity of the original samples (before soil burial) increased at higher

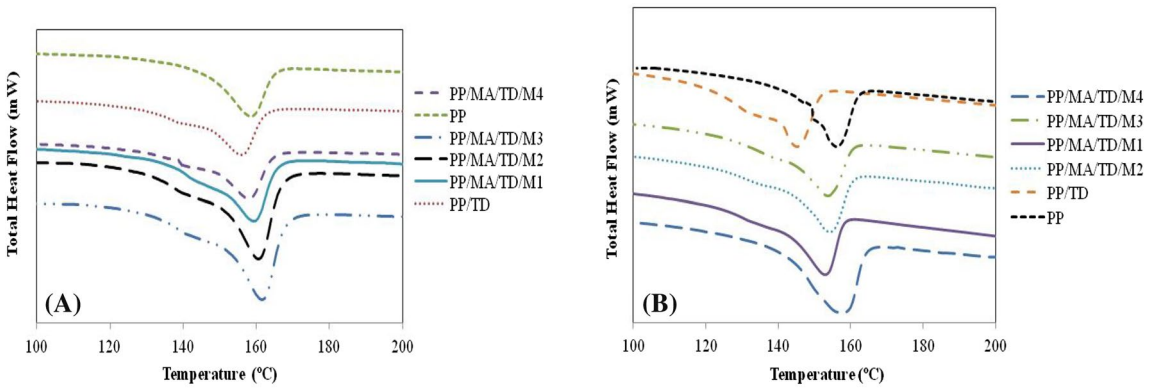

Fig. 1 DSC thermograms for all samples **a** samples before soil burial and **b** samples after soil burial

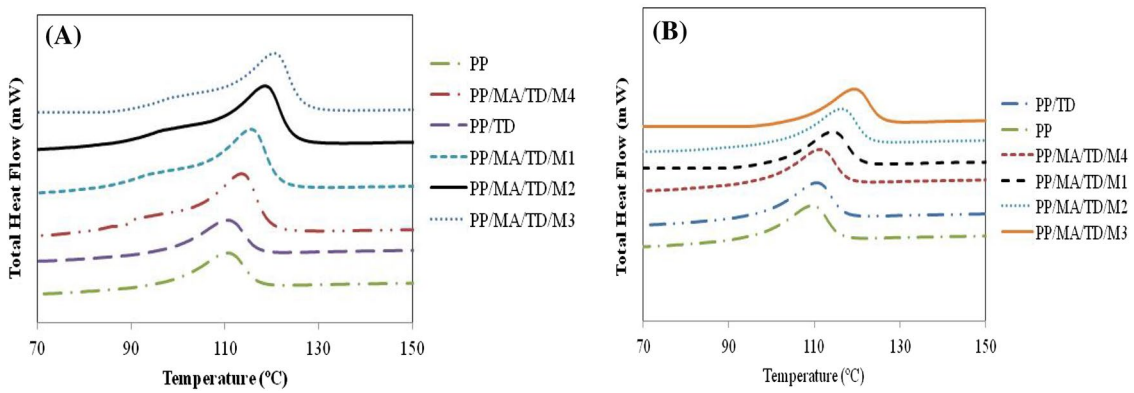

Fig. 2 DSC cooling curves for all samples **a** samples before soil burial and **b** samples after soil burial

Table 3 Thermal properties for all samples by DSC

Designations	Original sample before soil burial			Samples after soil burial for period of 6 months		
	T_m (°C)	T_c (°C)	X^*_c (%)	T_m (°C)	T_c (°C)	X^*_c (%)
PP	158	110	50.2	157	110	49.7
PP/TD	156	111	47.3	146	110	44.8
PP/MA/TD/M1	159	114	55.6	152	113	53.5
PP/MA/TD/M2	160	116	56.7	153	115	54.6
PP/MA/TD/M3	161	118	57.8	155	116	55.6
PP/MA/TD/M4	158	113	46.2	157	112	48.3

*The effect of MMT weight has been deducted

T_m melting temperature, T_c crystallization temperature, X_c crystallinity

MMT content. This increase of crystallinity indicates that the presence of MMT platelets promotes crystallization of PP, and this could suggest that the nanoclay acts as a nucleating agent. Previous studies [24] reported similar observation of increase in crystallinity with increasing MMT content in the polymer matrix. However, slight decrease of crystallinity was observed at 4 phr MMT content. The decrease in crystallinity with 4 phr MMT filled PP nanocomposite might be due to agglomeration of MMT at higher loadings, which could reduce the available surface for nucleation of PP crystals.

On the other hand, as shown in Fig. 1b and Table 3, samples subjected to a subsequent soil burial test for a period of 6 months have a different thermal behavior in terms of

melting and degree of crystallinity compare to its respective samples before the soil burial process. For instance, a shift of the DSC traces toward lower melting temperature was noted and observed after 6 months of soil burial, suggesting that the crystalline phase of polypropylene was affected during oxo-biodegradation process. Hence, this could have an influence on the melting temperature and leads to a decrease in the melting temperature. Furthermore, this decrease in melting temperature is more pronounced with the PP/TD sample, which does not contain MMT, where it decreased from 156 to 146 °C that is about 10 °C lower; this could be due to the faster oxo-biodegradation processes for this sample. It is interesting to note that samples with lower MMT content have reduced melting temperature after soil burial exposure compared to its respective samples, while no significant change in melting temperature was observed on the neat PP after 6 months of soil burial. This result indicates the evidence that addition of pro-degradant additive to the blend influences the degradation process of PP, and the incorporation of MMT to PP could compromise the degradation process of PP, and has an adverse impact on the degradation process. A similar trend of melting temperature decrease during biodegradation in soil with PP samples containing pro-degradant additive was reported previously [37, 46]. In terms of degree of crystallinity, trend of decrease was observed compare to the original samples (before soil burial) for each respective sample, it decreased slightly about 2 to 3% over the period of 6 months during incubation time in soil. This further decrease in crystallinity could be attributed to the biodegradation occurring in the amorphous phase due to the overall degradation process. Similarly, it is also noted the influence of pro-degradant additive is more pronounced for less MMT containing samples, where a lower degree of crystallinity are observed.

As shown in Fig. 2a, the crystallization temperature (T_c) of PP/MMT nanocomposites were higher than that of neat PP, which means increasing MMT content increases T_c from 110 °C of neat PP to 118 °C of PP/MA/TD/M3 for samples before soil burial, this is in agreement with literature [47–49]. This increase of T_c could indicate that MMT was effective in nucleating crystal. On the other hand, as shown in Fig. 2b and Table 3, samples subjected to a subsequent soil burial test for a period of 6 month have shown similar trend of T_c increase from 110 to 116 °C of neat PP and PP/MA/TD/M3 samples respectively. However, slight drop of crystallization temperature, about 2 °C, was observed after 6 month of soil burial samples compared to its respective samples before soil burial. This decrease of T_c suggests that the crystalline phase of polypropylene is affected during oxo-biodegradation process. It is also noted that no change in T_c was observed on the neat PP after 6 months of soil burial, and decrease in T_c was observed for 4 phr MMT content, which could be due to agglomeration of MMT at higher loadings as discussed earlier.

Thermogravimetric Analysis (TGA)

Thermal stability for all samples, before and after the soil burial, was investigated with TGA analysis and tabulated in Table 4. The onset temperatures ($T_{10\%}$) of 10% weight loss deviation from the base line (T_{10}) were used as the indicator of the compound's thermal stability. Figure 3a shows the TGA results for all samples before soil burial. As shown in Fig. 3a, PP nanocomposites show overall higher thermal stability compared to neat PP. The onset temperature ($T_{10\%}$) values of neat PP occurs at about 436 °C, while that of 1, 2, 3 phr MMT contents are increased by 6 °C (442 °C), 11 °C (447 °C) and 14 °C (450 °C) respectively. The incorporation of MMT nanoclay into PP matrix caused a significant improvement in the initial thermal stability of PP nanocomposites, which is clearly shown in Fig. 3a. This thermal stability improvement by MMT nanoclay could be attributed to because of nanoclay acting as a great insulator, mass transfer barrier, and like a shield for polymer from oxygen, thus increasing its thermal stability [50]. For instance, the decomposition temperature of neat PP sample at 10% was found to be 436 °C, while at 3 phr of MMT content it was

Table 4 TGA results for all samples

Designations	Sample decomposition temperature before soil burial			Sample decomposition temperature after soil burial		
	Weight loss,(T10%), (ºC)	DTG (Tmax), (ºC)	Residual (%)	Weight loss,(T10%), (ºC)	DTG (Tmax), (ºC)	Residual (%)
PP	436	461	0	435	460	0
PP/TD	412	462	1.5	395	430	1.2
PP/MA/TD/M1	442	470	2.5	425	455	2.4
PP/MA/TD/M2	447	475	3.7	430	461	2.5
PP/MA/TD/M3	450	496	4.6	443	476	4.3
PP/MA/TD/M4	442	486	4.8	445	468	4.5

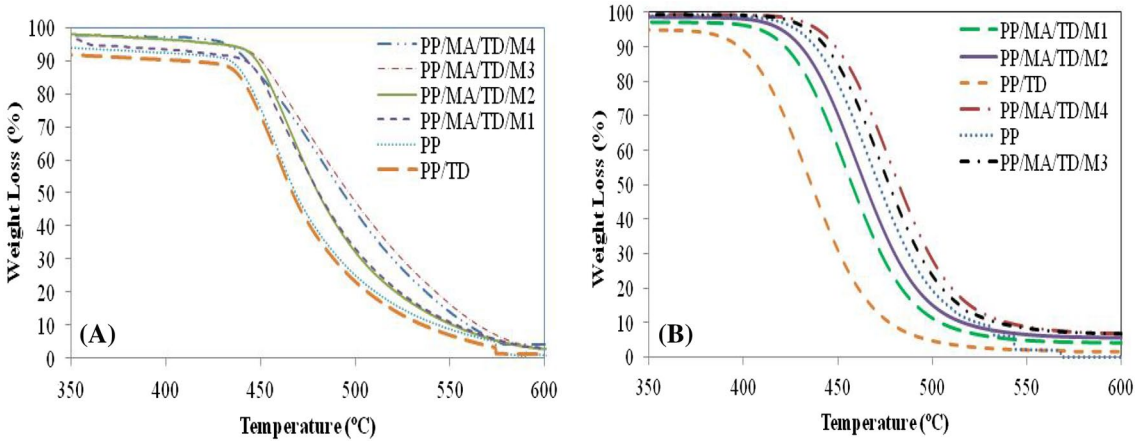

Fig. 3 TGA curves for all samples: **a** before soil burial samples and **b** after soil burial samples

450 °C with an increment of 14 °C improvement. However, at 4 phr of MMT content, a slight decrease of decomposition temperature was observed, which indicates that the composites reached a saturation point and an agglomeration at higher MMT contents occurred; a similar and consistent trend of behavior was observed also in the mechanical properties in the earlier discussions. On the other hand, the (PP/TD) sample had the lowest thermal stability compared to all other samples; this could be due to the addition of pro-degradant additive, which could initiate the accelerating rate of oxo-biodegradation process. And also no MMT nanoclay and PP-g-MAH compatibilizer content in this sample, which would have improved thermal stability properties. Therefore, these results indicate that the increase in the thermal stability of PP samples observed is mainly due to the addition of MMT nanoclay to PP matrix. Similar trend was observed by others [19] who reported that nanoclays such as MMT have good thermal stability and it can improve polymer thermal stability.

Similarly, all samples subjected to the soil burial test for a period of 6 months were also characterized by using TGA, and shown in Fig. 3b. The thermal degradation results for soil burial samples show that the addition of pro-degradant additive to the PP and its nanocomposites has decreased the thermal stability of neat PP at onset temperatures of 10% due to oxo-biodegradation process. It is worth mentioning that this decrease was more obvious for the PP sample containing only pro-degradant additive, sample (PP/TD), where decomposition temperature decreased from 412 °C (before soil burial) to 395 °C (after soil burial), which is about 17 °C as shown in Fig. 3b, followed by the samples with less MMT content, such as 1 and 2 phr, which have a lower decomposition temperature than neat PP. This result clearly indicates the significant influence of pro-degradant additive on the degradation process of virgin PP as it accelerates the oxo-biodegradation process of PP.

It is also noted that samples with MMT content of 1 and 2 phr (i.e., PP/MA/TD/M1 and PP/MA/TD/M2) respectively have achieved lower decomposition temperature compared to the neat PP and other nanocomposites (MMT content of 3 and 4 phr). It could be concluded that a lower thermal stability of these samples after soil burial is due to the existence of pro-degradant additive (TDPA) in the blend and lower loading amount of MMT content. Therefore, this combination of TDPA additive with less MMT content could contribute for accelerating faster degradation process of PP significantly, and further proves that pro-degradant additive is more effective for samples with less MMT content.

The temperatures corresponding to maximum decomposition temperature (T_{max}) were determined from the derivative thermogravimetry (DTG) curves given in Fig. 4 and the results obtained were tabulated in Table 4. The peak degradation temperature shown in Fig. 4 corresponds to the weight loss rate where the maximum degradation occurs. As shown Fig. 4a for samples before soil burial, the maximum decomposition temperatures (T_{max}) of neat PP and PP/TD samples are almost similar at 461 and 462 °C respectively, while T_{max} of other nanocomposite samples are higher due to the MMT content in the PP matrix, for instance at 3 phr of MMT content, T_{max} occurs at about 496 °C. Besides, T_{max} value of 3 phr MMT content is improved by 35 °C compared to that of neat PP. Therefore as discussed earlier the thermal stability of the PP is significantly enhanced by the addition of MMT nanoclay; and these results are in agreement with the previous studies [19]. However, for soil buried samples as shown in Fig. 4b were found to have further changes in thermal stability upon the incubation time in soil clearly indicating that the T_{max} of all samples were decreased, which could mean faster decomposition. However, no significant change of neat PP sample was observed. It is also noted that the decrease of

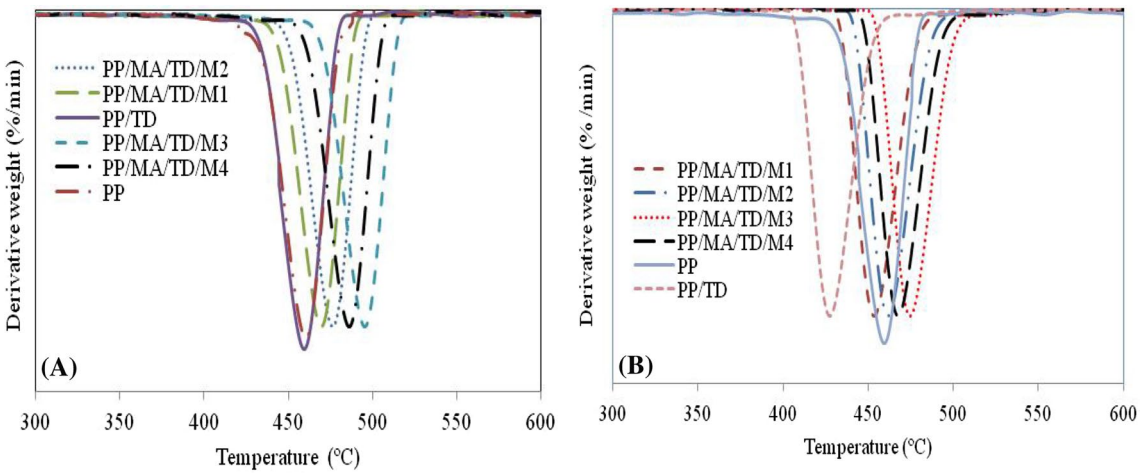

Fig. 4 DTG curves for all samples: **a** before soil burial samples and **b** after soil burial samples

T_{max} is more significant in PP/TD sample, where T_{max} was decreased from 462 to 430 °C, then followed by PP/MA/TD/M1, PP/MA/TD/M2 and PP/MA/TD/M3 respectively compared to neat PP. As previously mentioned, this could be attributed the existence of the pro-degradant additive in the PP matrix, which accelerates the degradation process. Similar trend of changes in the thermal stability with the incubation time in soil was also reported by others [37]. These results are in good agreement with DSC analysis earlier and further emphasize the influence of pro-degradant additive on the degradation process.

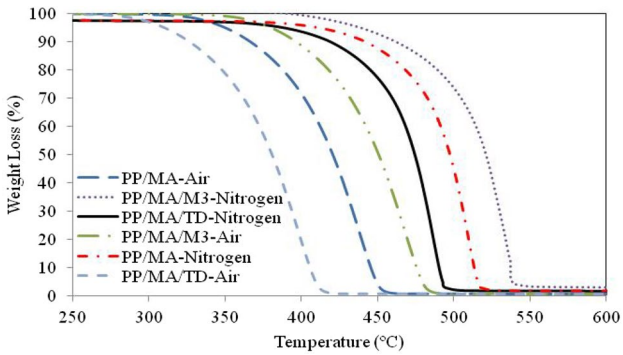

Fig. 5 TGA curves for the thermal decomposition of samples in air and nitrogen

Effect of TDPA Additive and MMTnanoclay on Thermal Degradation Process

To investigate the influence of each pro-degradant (TDPA) additive and MMT nanoclay on the thermal stability and degradation process, further test has been done by using thermogravimetric analysis (TGA) in both inert nitrogen and air atmosphere conditions at a heating rate of 10 °C min^{-1} for thermal and oxidative stability analysis. Samples PP/MA (PP and PP-g-MAH), PP/MA/TD (PP, PP-g-MAH and TDPA) and PP/MA/M3 (PP, PP-g-MAH and MMT) has been compounded and tested; to clarify which additive (TDPA or MMT) has more influence on thermal degradation behavior.

Figure 5 shows the TGA scans of PP/MA, PP/MA/TD and PP/MA/M3 samples degraded in Air and nitrogen. As shown in Fig. 5, samples degrade at lower temperature under air than under nitrogen, and it is particularly notable sample (PP/MA/TD) which contains pro-degradant additive degrades faster than other samples both in air and nitrogen. As clearly shown in Fig. 5 and Table 5, the onset temperature (temperature at 10% weight loss, $T_{10\%}$) was decreased for sample (PP/MA/TD) compared to sample (PP/MA/M3) by 70 and 50 °C under air and nitrogen respectively due to presence of TDPA additive in sample PP/MA/TD. It is also noted that PP-g-MAH compatibilizer slightly improved thermal properties of the composites; for instance the onset temperature for samples PP and PTD was 436 and 412 °C respectively as shown in Fig. 3a and Table 4, while onset temperature for samples PP/MA and PP/MA/TD was 440 and 416 °C respectively as shown in Fig. 5 and Table 5, which is about 3 to 4 °C degree improvement. However, sample PP/MA/TD/M3 which contains pro-degradant additive has onset temperature of 450 °C (Fig. 3a; Table 4) compared to 460 °C of sample PP/MA/M3 (Fig. 5; Table 5), which has decreased about 10 °C due to the existence of TDPA additive in the nanocomposite. The above results indicate that pro-degradant additive accelerates thermal degradation process compared to MMT nanoclay.

Similarly, the mass loss between 300 and 400 °C for all samples was also evaluated and tabulated in Table 5, and it was observed to increase as a function of pro-degradant additive (TDPA), clearly indicating accelerated degradation

Table 5 Sample degradation temperature and mass loss between 300–400ºC

Samples	Under Air			Under Nitrogen		
	Weight loss, (T10%), (ºC)	Mass loss, 300–400 °C (%)	Residual (%)	Weight loss, (T10%), (ºC)	Mass loss, 300–400 °C, (%)	Residual (%)
PP/MA	365	28	0.6	440	1.6	1.8
PP/MA/TD	326	78	1.0	416	3.5	2.3
PP/MA/M3	396	11.3	1.2	460	1.0	3.5

of composite in the presence of TDPA additive both in air and nitrogen. For instance under nitrogen, mass loss for samples PP/MA/TD and PP/MA/TD/M3 (Fig. 3a) was 3.5% and 2.1% respectively, while for sample PP/MA/M3 was 1%, which indicates the effects of TDPA additive on thermal degradation process was more pronounced compared to MMT nanoclay and it could cause faster degradation. The mass loss in the PP/MA sample as compared to PP/MA/M3 was also slightly increased, but was much lower than sample PP/MA/TD due to effect of pro-degradant additive. These results indicated that the TDPA additive contributed more efficiently to the thermal degradation process of the nanocomposites, while MMT nanoclay was detrimental to degradation process.

Finally it could be concluded that, the addition of MMT nanoclay filler into composite improved and enhanced thermal stability significantly due to reinforcement effect, while the addition of TDPA additive into composite reduced the thermal stability indicating that the MMT nanoclay filler and TDPA additive may have opposite synergistic effects on the thermal property enhancement. Further investigation of synergistic effects is still ongoing work in the lab.

Oxo-Biodegradability and Soil Burial Analysis

Simple soil burial test was conducted in order to investigate the actual effect of a normal composting environment on all the samples. In this paper, oxo-biodegradability was tested by using natural soil burial which is similar to the normal surrounding environment [51]. The percentage weight loss for all samples through oxo-biodegradation after soil burial, for a period of 6 months is presented in Fig. 6. As shown in Fig. 6, except for pure PP, which does not show any degradation after 6 months, PP/TD and PP nanocomposites were gradually degraded with time, particularly for lower MMT content nanocomposite samples.

It can be observed that the blending of pro-degradant additive (TDPA) into PP had a significant role in accelerating the oxo-biodegradation process of neat PP during the incubation period. For instance, as shown in Fig. 6, there is a sharp increase in weight loss for the sample (PP/TD) due to oxo-biodegradation, which attains weight loss of more than 4% for a period of 6 months compared to neat

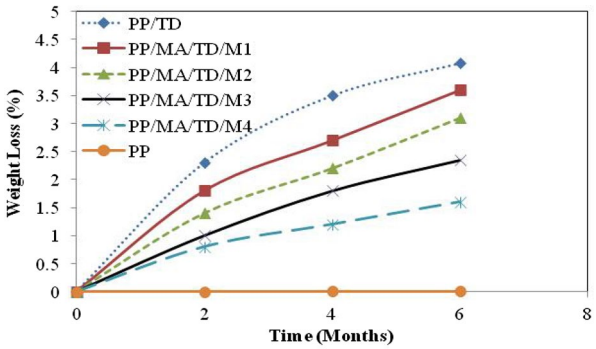

Fig. 6 Percentage weight loss for all samples after soil burial for 6 month

PP. This can be attributed the synergetic effect of heat exposure and biotic degradation, as a result of the activity of the soil microorganisms, which could accelerate the extent of the degradation process of the PP samples containing pro-degradant additive, which is main driving force for degradation process. It is also possible that the extreme heat here in Kuwait (summary time) during soil burial testing could be a contributing additional factor for the sample degradation process and weight loss. For neat PP sample, no significant change of degradation was observed during that period of 6 month. As shown in Fig. 6, increasing MMT content from 1 phr to 4 phr slightly reduced the weight loss and oxo-biodegradation rate of PP from 3.5 to 1.5%, respectively, for the 6 month outdoor exposure period. Therefore, increasing MMT content was detrimental to the degradation process, which means the more MMT content in the sample, the less weight loss of the sample was observed during soil burial test, which could eventually lead to a lower oxo-biodegradation rate of PP. This could be attributed that the presence of dispersed MMT layers with large aspect ratio had hindered the microorganism diffusion through the matrix, where more MMT layers act like a barrier in higher concentrations, which will result a lower diffusivity of water and microorganisms into the polymer matrix, thus reducing its degradability. The trend is consistent with the results reported by others [24, 52, 53], which revealed the slow degradation rate of polymer in the presence of MMT nanoclay filler. This result

of oxo-biodegradation further reveals the significant influence of TDPA additive on PP oxo-biodegradation process; and it is supported by the earlier analysis of DSC and TGA results.

Oxygen Permeability Analysis

Generally, it is believed that the addition of nanoparticles in the polymer matrix would enhance its barrier properties by forcing the gas molecules to follow a more tortuous path as they diffuse through the nanocomposite sample. This phenomenon is more pronounced and significant when fillers used are of nanometer size with high aspect ratio, since permeability depends on the aspect ratio of the clay layers. Therefore, researchers, such as Avella et al. [54], reported that nanofillers, particularly calcium carbonate, reduce the permeability to both oxygen and carbon dioxoide, and concluded that the nanofillers were responsible for higher barrier properties improvements. A similar trend of behavior was observed in this study.

The permeability results for all samples are tabulated in Table 6, while Fig. 7 shows the permeability versus samples with different MMT content. As shown both in Table 6 and Fig. 7, the permeability of oxygen decreased with increasing MMT nanoclay content. For instance, the 1 phr composition showed marginal reduction of about 6%, while 2 phr and 3 phr reduced permeability about 20 and 39%, respectively, compared to neat PP. Finally, the oxygen permeability at MMT content of 4 phr was reduced by almost 46% compared to neat PP. This reduction of PP permeability could be attributed to the nature of MMT nanoclay layers, as they themselves are unreceptive and impervious to oxygen, providing barrier resistance.

It is notable that the volume occupied by the clay and amount of clay influenced the actual three-dimensional arrangement and dispersion. For instance, at low concentrations of clay (1 phr), permeability decrease was not significant indicating that there was not enough or sufficient platelets to provide required resistance to permeability [55]. While at higher concentration of nanoclay, permeability decreased significantly from 6 to 46%. Hence, it

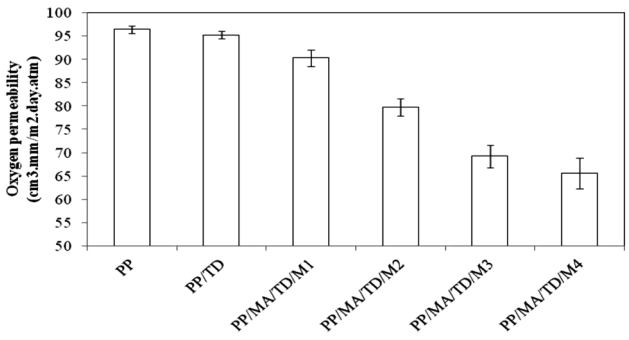

Fig. 7 Oxygen permeability results for all samples

could be concluded that the change in oxygen permeability of nanocomposites was controlled by the nanoclay content and microstructure. It is possible that the more tortuous path needed for the passage of the gas molecules through the polymeric film is the cause of this, due to the impermeability of silica particles, and when dispersed into polymer, nanoclays were effective at improving barrier properties of polymeric material [56]. It is noted that the sample PP/TD has almost similar permeability value with neat PP; and no significant change was observed. Therefore, the addition of pro-degradant additive had no significant influence on the barrier properties. The overall change in the oxygen permeability of nanocomposites was apparently controlled by the MMT nanoclay content, which proves that platelet structure and dispersion were necessary in order to achieve permeability reduction.

X- ray Diffraction (XRD) Analysis

The structure and morphology of PP nanocomposites was examined using XRD technique and its analysis was carried out to confirm the formation of intercalated/exfoliated nanocomposite. The XRD pattern of MMT and PP nanocomposites is shown in Fig. 8 and all corresponding results are tabulated in Table 7. The (001) diffraction peak in pure MMT was registered at $2\theta = 3.1°$, which corresponds to an

Table 6 Tabulated oxygen permeability results for all samples

Sample	MMT (Phr)	Oxygen permeability [cm3.mm/m2.day.atm]				
		Sample 1	Sample 2	Sample 3	Average	Standard deviation
PP	0	97.2	95.5	96.6	96.4	0.8
PP/TD	0	96	94.5	95	95.2	0.8
PP/MA/TD/M1	1	88.5	90.3	92	90.3	1.8
PP/MA/TD/M2	2	80	81.4	77.8	79.7	1.8
PP/MA/TD/M3	3	71.2	70	66.5	69.2	2.4
PP/MA/TD/M4	4	64.5	69.3	63	65.6	3.3

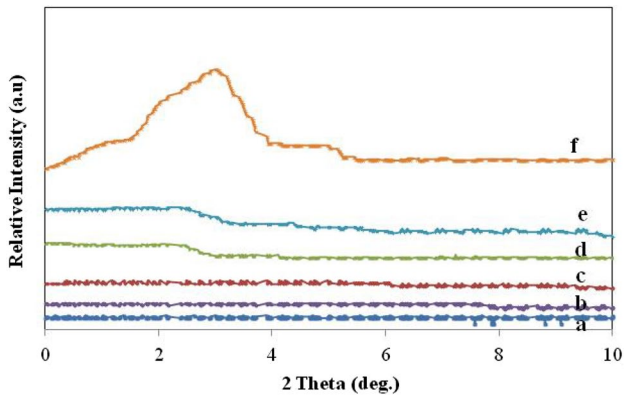

Fig. 8 XRD results for PP and its nanocomposites

Table 7 The 2θ angle and d-spacing of MMT and PP nanocomposites

Designations	MMT (Phr)	2θ angle (°)	d-spacing (nm)
PP	0		
PP/MA/TD/M1	1	No peak	
PP/MA/TD/M2	2	No peak	
PP/MA/TD/M3	3	2.5	3.5
PP/MA/TD/M4	4	2.5	3.5
Pure MMT	100	3.1	2.8

interlayer spacing of nanoclay (d-spacing) of 2.8 nm (calculated from Bragg's diffraction law shown in Eq. 1).

Figure 8 also illustrates a small bulge of diffraction peak of 2θ at 2.5° with 3 and 4 phr addition of MMT in PP nanocomposite. The weak peaks correspond to the interlayer spacing of stacked MMT layers with nanoclay (d-spacing) of 3.5 nm for both 3 and 4 phr MMT content as shown in Table 7. Hence, the interlayer spacing of nanoclay is increased by about 0.7 nm due to the presence of matrix polymer in the interlayer region of nanoclay and it is evidence that PP polymer chains were intercalated, and the structure is a typical intercalated structure. The increase in interlayer spacing of MMT could be due to the organic modification of MMT which provides the possibility for PP chains to diffuse between the layers during processing. Therefore, it can be noted that at higher MMT concentrations (3 and 4 phr), more agglomeration of MMT in the polymer matrix were observed as also shown by TEM images. This could be possible due to the filler–filler interactions of the MMT, resulting in agglomerates, which as a result restricted the delamination of the MMT.

It is interesting to note that the XRD pattern of PP nanocomposites with 1 and 2 phr MMT content (Fig. 8) do not show peaks, and there is an absence of a diffraction peak. This suggests that the parallel form of stacking of the MMT was totally disrupted. It also further indicates the scattering and dispersion of the MMT nanolayers within the PP matrix with the formation of fully exfoliated nanostructure for PP/MA/TD/M1 and PP/MA/TD/M2 samples.

Transmission Electron Microscope (TEM) Analysis

Figure 9 illustrates the TEM results of PP nanocomposites with different MMT contents from 1 to 4 phr. The grey areas in Fig, 9 represent MMT layers in PP matrix. As shown in Fig. 9a, b the layered MMT in both PP/MA/TD/M1 and PP/MA/TD/M2 for 1 and 2 phr respectively show the dispersion of MMT in PP matrix and no significant agglomeration of MMT was visible in the TEM image (Fig. 9a, b). This could mean that layered MMT in PP/TD/MA/M1 and PP/TD/MA/M2 are exfoliated, which is consistent to the XRD patterns observed earlier (Fig. 8).

Figure 9c, d show the dispersion of MMT in the PP matrix for PP/MA/TD/M3 and PP/MA/TD/M4 samples with addition of 3 and 4 phr MMT respectively. It could be seen that at higher MMT loading (4phr), more darker platelets appeared, which means more agglomeration of MMT were visible in the nanocomposites. This could be due to the filler–filler interactions of the MMT resulting agglomeration of MMT, which as a result decreases the degree of exfoliation. It could be concluded that TEM images have revealed that the MMT layers had agglomerated at higher MMT content (4 phr), which is consistent with XRD results reported earlier. This could be the possible reason for the decrease in the mechanical and thermal properties observed earlier for sample PP/MA/TD/M4; similar trend was reported in the literature by [57].

Scanning Electron Microscopy (SEM) Analysis

Figure 10 shows SEM micrographs for all samples before and after composting for a period of 6 months to simulate the oxo-biodegradation process in a common disposal environment.

As shown in Fig. 10, after outdoor exposure and composting, the surface of the soil buried samples have trace of shrinkage and roughness due to degradation process compared with the same samples before soil burial at the initial time. The degradation trace is more significant for the PP/TD and PP/MA/TD/M1 samples, which contains only prodegradant additive and minimum amount of MMT respectively. It is clearly shown the deterioration of the sample surface, which demonstrates visible and remarkable surface degradation sign. Similar observation was reported in the literature [36, 58]. However, for the neat PP sample, no significant surface degradation was observed.

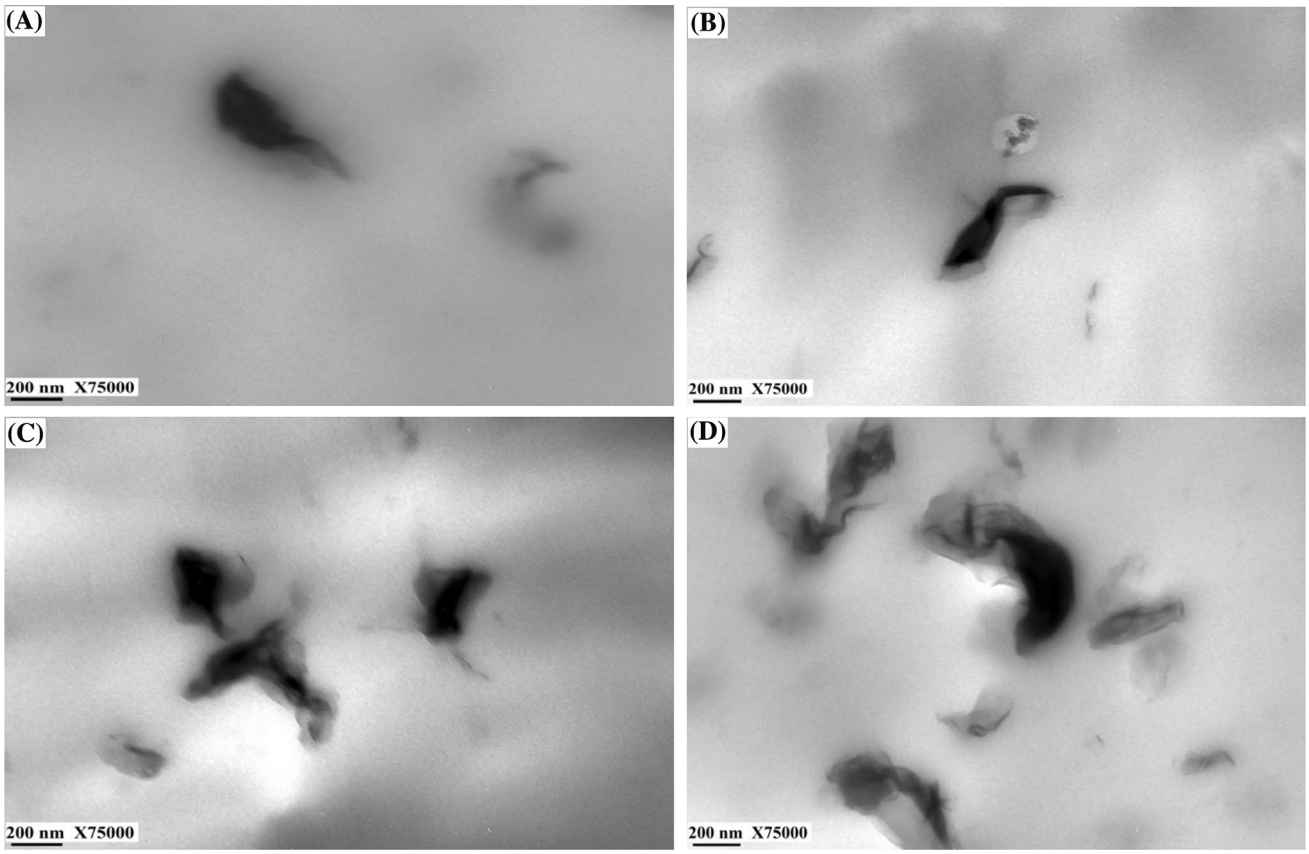

Fig. 9 TEM micrographs (X75000) of PP nanocomposites with different MMT loading: **a** PP/MA/TD/M1, **b** PP/MA/TD/M2, **c** PP/MA/TD/M3 and **d** PP/MA/TD/M4

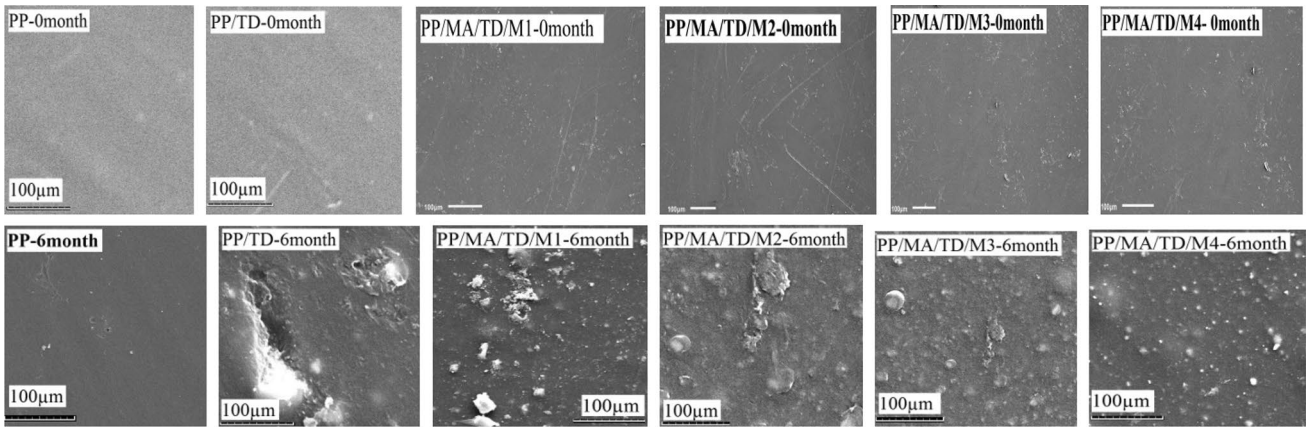

Fig. 10 SEM micrographs of the surface of the samples before (0 month) and after degradation (6 month) of simulated soil

Conclusion

Polypropylene/MMT nanocomposites compatibilized with PP-g-MA, and blended with a pro-degradant additive were successfully prepared by melt mixing using a twin-screw extruder. The mechanical, thermal, barrier, oxo-biodegradation, and morphological properties of PP and its nanocomposites were investigated and reported. The tensile strength and Young's modulus of neat PP were improved with increasing loadings of MMT by 45% and 27% respectively. However, the tensile and Young's modulus decreased with further addition of MMT at 4 phr.

Thermal analysis through DSC revealed that melting temperature (T_m), percentage crystallinity (X_c) and crystallization temperature (T_c) of PP increased slightly with increasing MMT content for original samples (before burial). This increase of crystallinity indicates the presence of MMT platelets, which promotes crystallinity of PP. However, slight decrease of all these parameters was observed after 6 month period of soil incubation, and due to oxo-biodegradation it was found that soil buried samples had a reduction of crystallinity, crystallization temperature and melting point compared to its respective samples. TGA results revealed that the incorporation of MMT had improved the thermal stability of PP. However, it is concluded that after a 6 month period of soil burial and outdoor environment exposure, significant changes in the thermal properties, and reduced thermal stability were detected in PP samples containing pro-degradant additive compared to neat PP, particularly at lower MMT loading (1 and 2 phr). Furthermore, these changes are more pronounced with PP/TD sample, which does not contain MMT filler. These results indicate that the pro-degradant additive (TDPA) can promote oxo-biodegradation of PP during soil burial. For oxo-biodegradability test, the addition of pro-degradant additive showed an improvement in the oxo-biodegradability of PP and nanocomposites; particularly sample PP/TD, which attains weight loss of more than 4% for a period of 6 months compared to neat PP. However, the incorporation of higher MMT nanoclay content to PP could compromise degradability of the nanocomposites. It was found that, increasing MMT content from 1 phr to 4 phr slightly reduces weight loss and oxo-biodegradation rate of PP from 3.5 to 1.5%, respectively, for the 6 month outdoor exposure period, which means that increasing MMT content was detrimental to oxo-degradation process, particularly at higher MMT content of 3 and 4 phr. The permeability of PP decreased (ca 46%) with increasing MMT content due to the longer transport pathway; hence, the change in oxygen permeability of PP nanocomposite was controlled by the MMT content, indicating that platelet structure and dispersion were important in obtaining permeability reduction. The XRD and TEM results showed and proven the formation of exfoliated nanocomposites for MMT loading of 1 phr and 2 phr, while agglomeration of MMT layers was observed at 4 phr MMT content. According to SEM results, the soil buried samples show rough and deterioration on the sample surface compared to original sample due to degradation. Hence, changes both thermal stability and morphological properties of the PP matrix during soil incubation period were controlled by pro-degradant additive. It can be concluded that, the potential of this pro-degradant additive (TDPA) in producing environmentally degradable nanocomposites has been confirmed. However further research is needed in order to make a right balance between barrier and degradability properties when MMT and pro-degrant additives are used together as a blend; and further future work for investigating the possible synergetic effects of MMT, PP-g-MAH and TDPA would be recommended.

Acknowledgements The authors would like to thank the Kuwait Institute for Scientific Research (KISR) for providing the grant (project PC014K) that has made this research work possible. The authors also would like to express gratitute to Prof. Dr. AbdelMageed Safer, Miss Ahlam Al Kadi and Miss Nisha Philip from Kuwait University, Faculty of Science at Nanoscopy Science Center for providing TEM facility to analysize our nanocomposite samples.

References

1. Paul DR, Robeson LM (2008) Polymer nanotechnology: Nanocomposites. Polymer 49(15):3187–3204
2. Ciardelli F, Coiai S, Passaglia E, Pucci A, Ruggeri G (2008). Nanocomposites based on polyolefins and functional thermoplastic materials. Polym Int 57 (6): 805–836.
3. Pettarin V, Brun F, Viana JC, Pouzada AS, Frontini PM (2013) Toughness distribution in complex PP/nanoclay injection mouldings. Compos Sci Technol 74:28–36
4. Dehaghani HE, Barikani M, Khonakdar HA, Jafari SH, Wagenknechy U, Heinrich G (2015) On O_2 gas permeability of PP/PLA/clay nanocomposites: A molecular dynamic simulation approach. Polym Test 45:139–151
5. Pluta M, Piorkowska E (2015) Tough and transparent blends of polylactide with block copolymers of ethylene glycol and propylene glycol. Polym Test 41:209–218
6. Gooddarzi V, Jafari SH, Khonahdar HA, Ghalei B, Morttazavi M (2013) Assessment of role of morphology in gas permselectivity of membranes based on polypropylene/ethylene vinyl acetate/clay nanocomposite. J Membr Sci 445:76–87
7. Shields RJ, Bhattacharya D, Fakirov S (2008). Oxygen permeability analysis of microfibril reinforced composites from PE/PET blends. Composites A 39: 940–949.
8. Farsani RE, Khalili SHR, Hedayatnasab Z, Soleimani N (2014). Influence of thermal conditions on the tensile properties of basalt fiber reinforced polypropylene-clay nanocomposites. Mater Des, 53: 540–549.
9. Fuad MYA, Hanim H, Zarina R, Ishak ZAM, Hassan A (2010). Polypropylene/calcium carbonate nanocomposites-effects of processing techniques and maleated polypropylene compatibiliser. Express Polym Lett 4 (10): 611–620.
10. An JE, Jeon GW, Jeong YG (2012). Preparation and properties of polypropylene nanocomposites reinforced with exfoliated graphene. Fibers Polym 13 (4): 507–514.
11. Komatsu LGH, Oliani WL, Lugao AB, Parra DF (2014). Environmental ageing of irradiated polypropylene/montmorillonite nanocomposites ontained in molten state. Radiat Phys Chem 97: 233–238.
12. Yuan Q, Misra RDK (2006) Impact behaviour of clay reinfornced polypropylene nanocomposites. Polymer 47:4421–4433
13. Saminathan K, Selvakumar P, Bhatnagar N (2008) Fracture studies of polypropylene/nanoclay composite. Part I: Effect of loading rates on essential work of fracture. Polym Test 27:296–307
14. Eslami FR, Hedayatnasab Z, Khalili SM, Soleimani N. (2012). Mechanical characterization of nanoclay reinforced polypopylene composites at high temperature subjected to tensile loads. Adv Mater Res, 488–489: 567–5671.

15. Nguyen QT, Baird DG (2006). Preparation of polymer-clay nanocomposites and their properties. Adv Polym Technol 25 (4): 270–285.
16. Hambir S, Bulakh N, Jog JP (2002) Polypropylene/clay nanocomposites: effect of compatibilizer on the thermal, crystallization and dynamic mechanical behaviour. Polym Eng Sci42(9):1801–1807
17. Liborio P, Oliveira VO, Marques MDF (2015) New chemical treatment of bentonite for the preparation of polypropylene nanocomposites by melt intercalation. Appl Clay Sci 111:44–49
18. Sharma SK, Nayak SK (2009). Surface modified clay/polypropylene (PP) nanocomposites: Effect on physico-mechanical, thermal and morphological properties. Polym Degrad Stab 94: 132–138.
19. Fitaroni LB, Lima JAD, Cruz SA, Waldman WR (2015). Thermal stability of polypropylene – montmorillonite clay nanocomposites: Limitation of the thermogravimetric analysis. Polym Degrad Stab 111: 102–108.
20. Al-Malaika S, Sheena H, Fischer D, Masarati E (2013). Influence of processing and clay type on nanostructure and stability of polypropylene-clay nanocomposites. Polym Degrad Stab 98: 2400–2410.
21. Hu D, Chen J, Zhao L, Liu T (2015) Melting and non-isothrmal crystallization behaviours of polypropylene and polypropylene/montmorillonite nanocomposites under pressurized carbon dioxide. Thermochim Acta 617:65–75
22. Mans R, Huang CT, Quintela A, Rocha F, Detellier C (2015) Preparation and characterization of novel clay/PLA nanocomposites. Appl Clay Sci 115:87–96
23. Raquez JM, Habibi Y, Murariu M, Dubois P (2013). Polylactic (PLA) based nanocomposites. Prog Polym Sci 38 (10–11): 1504–1542.
24. Balakrishnan H, Masoumi I, Yussuf AA, Imran M, Hassan A, Wahit MU (2012). Ethylene copolymer toughened polylactic acid nanocomposites. Polym-Plast Technol Eng 51: 19–27.
25. Pisano C, Figiel L (2013) Modelling of morphology evolution and macroscopic behaviour of intercalated PET-clay nanocomposites during semi-solid state processing. Compos Sci Technol 75:35–41
26. Yang F, manitium M, Kriegel R, Kannan RM (2014) Stucture, permeability, and rheology of supercritical CO2 dispersed polystyrene-clay nanocomposites. Polymer 55:3915–3924
27. Tang Y, Hu Y, Song L, Zong R, Gui Z, Chen Z (2003). Preparation and thermal stability of polypropylene/montmorillonite nanocomposites. Polym Degrad Stab 82: 127–131.
28. Silvano JR, Rodrigues SA, Marini J, Brestas RES, Canevarolo SV, Carvalho BM, Pinheiro LA (2013). Effect of reprocessing and clay concentration on the degradation of polypropylene/montmorillonite nanocomposites during twin screw. Polym Degrad Stab 98: 801–808.
29. Baniasadi H, Ramazani ASA, Nikkhah SJ (2010). Investigation of in situ prepared polypropylene/clay nanocomposites properties and comparing to melt blending method. Mater Des 31: 76–84.
30. Chen J, Yu Y, Chen J, Li H, Liu D (2015). Chemical modification of palygorskite with maleic anhydride modified polypropylene: Mechanical properties, morphology, and crystal structure of palygorskite/polypropylene nanocomposites. Appl Clay Sci 115: 230–237.
31. Salehiyan R, Yussuf AA, Hanani NF, Hassan A, Akhbari A (2015) Polylactic acid/polycaprolactone nanocomposite: Influence of montmorillonite on mechanical, thermal, and morphological properties. J Elast Plast 47(1):69–87
32. Ammala A, Bateman S, Dean K, Petinakis E, Sangwan P, Wong S, Yuan Q, Yu L, Patrick C, Leong KH (2011). An overview of degradable and biodegradable polyolefins. Prog Polym Sci 36: 1015–1049.
33. Ojeda TFM, Dalmolin E, Forte MMC, Jacques RJS, Bento FM, Camargo FAO (2009). Abiotic and biotic degradation of oxo-biodegradable polyethylene. Polym Degrad Stab 94: 965–970.
34. Husarova L, Machovsky GP, Houser J, Koutny M (2010). Aerobic biodegradation of calcium carbonate filled polyethyelene film containing pro-oxidant additives. Polym Degrad Stab 95: 1794–1799.
35. Roy PK, Titus S, Surekha P, Tulsi E, Deshmukh C, Rajagopal C (2008). Degradation of abiotically aged LDPE films containing pro-oxidant by bacterial consortium. Polym Degrad Stab 93: 1917–1922.
36. Montagna LS, Forte MMC, Santana RMC (2013) Induced degradation of polypropylene with an organic pro-degradant additive. J Mater Sci Eng A3(2):123–131
37. Contat-Rodrigo L (2013). Thermal characterization of the oxo-degradation of polypropylene containing a pro-oxidant/pro-degradant additive. Polym Degrad Stab 98: 2117–2124.
38. Karian HG (2003) Handbook of polypropylene and polypropylene composites. Marcel Dekker, New York
39. Osman MA, Atallah A (2004). High density polyethyelene micro- and nanocomposites: effect of particle shape, size, and surface treatment on polymer crystallinity and gas permeability. Macro Rap Comm 25: 1540–1544.
40. Bagheriasl D, Carreau PJ, Dubois C, Riedl B (2015) Properties of polypropylene and polypropylene/poly(ethylene-co-vinyl alcohol) blend/CNC nanocomposites. Compos Sci Technol 117:357–363
41. Rosa DS, Bardi MAG, Calil MR, Guedes CGF, Ramires EC, Frollini E (2009) Mechanical, thermal and morphological characterization of polypropylene/biodegradable blends with additives. Polym Test 28(8):836–842
42. Chen L, Wong SC, Pisharath S (2003) Fracture properties of nanoclay-filled polypropylene. J Appl Polym Sci 88:3298–3305
43. Selvakumar V, Palanikumar K, Palanivelu K (2010) Studies on mechanical characterization of polypropylene/Na-MMT nanocomposites. J Min Mater Charac Eng 9(8):671–681
44. Chung YL, Ansari S, Estevez L, Hayrapetyan S, Giannelis EP, Lai HM (2010) Preparation and properties of biodegradable starch-clay nanocomposites. Carbohydr Polym 79:391–396
45. Bagheri-Kazemabad S, Fox D, Chen Y, Geever LM, Khavandi A, Bagheri R, Higginbotham CL, Zhang H, Chen B (2012) Morphology, rheology and mechanical properties of polypropylene/ethylene-octene copolymer/clay nanocomposites: effects of the compatibilizer. Compos Sci Technol 72:1697–1704
46. Fechine GJM, Rosa DS, Rezende ME, Demarquette NR (2009) Effect of UV radiation and pro-oxidant on polyethyelene biodegradability. Polym Eng Sci 49:123–128
47. Lee SY, Kang IA, Doh GH, Kim JS, Yoon HG, Wu Q (2008). Thermal, mechanical and morphological properties of polypropylene/clay/wood flour nanocomposies. Express Polym Lett 2 (2): 78–87.
48. Baniasadi H, Ramazani SA, Nikkhah SJ (2010). Investigation of in situ prepared polypropylene/clay nanocomposites properties and comparing to melt blending method. Mater Des 31: 76–84.
49. Prasad KH, Kumar MS (2011) Thermal characterization of PP/NA-MMT composite materials. J Mater Sci Eng 5:80–86
50. Sinha RS, Bousima M (2005). Biodegradable polymers and their layered silicate nanocomposites: in greening the 21st century materials world. Progr Mater Sci 50: 962–1079.
51. Yussuf AA, Massoumi I, Hassan A (2010) Comparison of polylactic acid/kenaf and polylactic acid/rise husk composites: the influence of the natural fibers on the mechanical, thermal and biodegradability properties. J Polym Environ 18:422–429

52. Chuayjuljit S, Hosililak S, Athisart A (2009) Thermoplastic cassava starch/sorbitol-modified montmorillonite nanocomposites blended with low density polyethylene: properties and biodegradability study. J Metal Mater Miner 19(1):59–65
53. Heydari A, Alemzadeh I, Vossoughi M (2014). Influence of glycerol and clay contents on biodegradability of corn starch nanocomposites. Inter J Eng 27 (2): 203–214.
54. Avella M, Cosco S, Di Lorenzo M, Di Pace E, Gentile G, Errico M (2006). iPP based nanocomposites filled with calcium carbonate nanoparticles: structure/properties relationships. Macromole Sympos 234 :156–162.
55. Faisant J, Ait-Kadir A, Bousmina M, Deschenes L (1998) Morphology, thermomechanical and barrier properties of polypropylene-ethylene vinyl alcohol blends. Polymer 3–9:533–545
56. Sinha RS, Okamoto M (2003). Polymer/layered silicate nanocomposites: a review from preparation to processing. Progr Polym Sci 28(11): 1539–1642.
57. Balakrishnan H, Hassan A, Wahit MU, Yussuf AA, Abdul Razak SB (2010). Novel toughened polylactic acid nanocomposite: mechanical, thermal and morphological properties. Mater Des 31: 3289–3298.
58. Montagna LS, Catto AL, Forte MMC, Santana RMC (2016). Biodegradation of PP films modified with organic pro-degradant: natural ageing and biodegradation in soil in respirometric test. Polyolefins J 3 (1): 59–68.